© 2023 Journal of Pharmacy & Pharmacognosy Research, 11 (5), 757-774, 2023
ISSN 0719-4250
https://jppres.com

DOI: https://doi.org/10.56499/jppres23.1652_11.5.757

*Original Article*

# Predicting anti-hyperuricemic and anti-gouty activities of fatty acids from *Limonia acidissima* L. fruit: *In silico-in vivo* study

[Predicción de la actividad anti-hiperuricémica y anti-gotosa de los ácidos grasos del fruto de *Limonia acidissima* L.: Estudio *in silico-in vivo*]

**Rika Yusnaini[1,2], Ikhsan[1,3], Salfauqi Nurman[4,5], Rinaldi Idroes[6,7], Teti Arabia[8], Nurdin Saidi[6], Rosnani Nasution[6*]**

[1]Graduate School of Mathematics and Applied Sciences, Universitas Syiah Kuala, Banda Aceh 23111, Indonesia.
[2]Department of Psychology and Nursing, Faculty of Medicine, Malikussaleh University, Lhokseumawe, 24351, Indonesia.
[3]Department of Surgery Tgk. Chik Di Tiro Hospital, Sigli 24116, Indonesia.
[4]Department of Agricultural Industrial Engineering, Faculty of Agricultural Technology, Universitas Serambi Mekkah, Banda Aceh 23245, Indonesia.
[5]Department of Ship Engineering, Politeknik Pelayaran Malahayati, Aceh Besar 23381, Indonesia.
[6]Department of Chemistry, Faculty of Mathematics and Natural Sciences, Universitas Syiah Kuala, Banda Aceh 23111, Indonesia.
[7]Department of Pharmacy, Faculty of Mathematics and Natural Sciences, Universitas Syiah Kuala, Banda Aceh 23111, Indonesia.
[8]Department of Agricultural, Universitas Syiah Kuala, Banda Aceh 23111, Indonesia.
*E-mail: rosnani@usk.ac.id

**Abstract**

*Context*: As of today, the knowledge of the role of nutraceuticals in treating metabolic diseases such as hyperuricemia is still limited.

*Aims*: To evaluate the mechanisms of anti-hyperuricemic and anti-gouty activity of *Limonia acidissima in silico* and *in vivo*.

*Methods*: *L. acidissima* fruits fine powder was macerated simultaneously using n-hexane, ethyl acetate, ethanol, and methanol sequentially. The structures of the GC-MS-identified phytocompounds were evaluated for their pharmacokinetic properties (SwissADME), traced for receptor targets (SEA Target), and converted to 3D structures and molecular anchoring (MOE software). Networking relationship analyses were performed using Cytoscape version 3.8.2. Anti-hyperuricemia effect was assessed with hyperuricemia rats induced by potassium oxonate. The anti-inflammatory effect was evaluated on acute gouty arthritis induced by monosodium urate (MSU) crystal.

*Results*: The predominant fatty acid contents (oleic acid, palmitoleic acid, and n-hexadecanoic acid) have satisfactory pharmacokinetic properties based on Lipinsky's rules. PPAR-γ, FABP3, OAT1, and OAT3 were revealed as targets for the fatty acid receptors. The highest interaction was obtained from oleic acid interaction with PPAR-γ (-12.54 kcal/mol) and FABP3 (-13.09 kcal/mol). The EEL 400 mg/kg effectively upregulated the protein levels of OAT1 ($p=0.001$) and OAT3 ($p=0.048$) in the kidneys of hyperuricemic rats. Moreover, EEL 400 mg/kg alleviated the swelling ($p<0.001$) and reduced inflammatory cell infiltration around the ankle joints in rats with acute gouty arthritis.

*Conclusions*: The networking analysis suggests that PPAR-γ and FABP3 could form an interaction to modulate XO directly. *L. acidissima* exhibited anti-hyperuricemic by regulating renal organic ion transporter expression and anti-gout arthritis effects by suppressing inflammation response.

*Keywords*: anti-inflammatory agents; urate transporters; uric acid.

**Resumen**

*Contexto*: A día de hoy, el conocimiento del papel de los nutracéuticos en el tratamiento de enfermedades metabólicas como la hiperuricemia es todavía limitado.

*Objetivos*: Evaluar los mecanismos de la actividad antihiperuricémica y anti-gotosa de *Limonia acidissima in silico* e *in vivo*.

*Métodos:* El polvo fino de los frutos de *L. acidissima* se maceró simultáneamente con n-hexano, acetato de etilo, etanol y metanol. Las estructuras de los fitocompuestos identificados por GC-MS se evaluaron en función de sus propiedades farmacocinéticas (SwissADME), se rastrearon en busca de dianas receptoras (SEA Target) y se convirtieron en estructuras tridimensionales y anclajes moleculares (software MOE). Los análisis de relación de redes se realizaron con Cytoscape versión 3.8.2. El efecto antihiperuricemia se evaluó con ratas hiperuricémicas inducidas por oxonato potásico. El efecto antiinflamatorio se evaluó en artritis gotosa aguda inducida por cristal de urato monosódico (MSU).

*Resultados*: Los contenidos predominantes de ácidos grasos (ácido oleico, ácido palmitoleico y ácido n-hexadecanoico) tienen propiedades farmacocinéticas satisfactorias basadas en las reglas de Lipinsky. PPAR-γ, FABP3, OAT1 y OAT3 se revelaron como dianas de los receptores de ácidos grasos. La mayor interacción se obtuvo de la interacción del ácido oleico con PPAR-γ (-12,54 kcal/mol) y FABP3 (-13,09 kcal/mol). Los 400 mg/kg de EEL aumentaron eficazmente los niveles proteínicos de OAT1 ($p=0,001$) y OAT3 ($p=0,048$) en los riñones de ratas hiperuricémicas. Además, EEL 400 mg/kg alivió la hinchazón ($p<0,001$) y redujo la infiltración de células inflamatorias alrededor de las articulaciones del tobillo en ratas con artritis gotosa aguda.

*Conclusiones*: El análisis en red sugiere que PPAR-γ y FABP3 podrían formar una interacción para modular XO directamente. *L. acidissima* mostró efectos antihiperuricémicos al regular la expresión del transportador renal de iones orgánicos y efectos antiartríticos por supresión de la respuesta inflamatoria.

*Palabras Clave*: ácido úrico; agentes anti-inflamatorios; transportadores de urato.

ARTICLE INFO
Received: April 7, 2023.
Accepted: July 30, 2023.
Available Online: August 23, 2023.

AUTHOR INFO
ORCID: 0000-0001-8781-1989 (RY) 0000-0003-2264-6358 (RI)
0000-0002-9073-9145 (I) 0000-0002-8356-8229 (TA)
0000-0002-2058-3288 (SN) 0000-0001-5372-5935 (RN)

## INTRODUCTION

Uric acid (UA) is the end product of purine metabolism in humans, where its excessive accumulation causes hyperuricemia exceeding its serum solubility limit (>6.8 mg/dL) (Strilchuk et al., 2019). Hyperuricemia is a major risk factor for gout arthritis, a condition with accumulation and deposition of monosodium urate crystals in joints, tendons, and surrounding tissues accompanied by sudden and intense pain, redness, swelling, and stiffness in the big toe, ankle, knee, elbow, wrist, and other joints (Cabău et al., 2020; Wu et al., 2019). Hyperuricemia is also associated with an increased risk of cardiovascular disease, chronic kidney disease, type 2 diabetes mellitus, hypertension, and metabolic syndrome (Ni et al., 2019; Wang et al., 2016). Due to its high contribution to morbidity and mortality, it is important to develop proper therapeutical agents for hyperuricemia and gout arthritis.

Excess production or low excretion of UA greatly affects the occurrence of hyperuricemia (Cui et al., 2020; Serrano et al., 2020). The production of UA is facilitated by xanthine oxidase (XO), which catalyzes the oxidation of hypoxanthine to xanthine concomitant to its conversion into UA (Sungthong et al., 2016). In addition, UA homeostasis is also influenced by the action of urate transporters in the excretion process through the kidneys (67-75%). Uric acid transporter 1 (URAT1) and glucose transporter 9 (GLUT9) assist UA reabsorption (Stewart et al., 2019). The organic anion transporter (OAT) is also a UA transporter, in which its dysfunction is associated with hyperuricemia and gout (Zhu et al., 2017).

The management of hyperuricemia is carried out by inhibiting the production and increasing the excretion of UA (Serrano et al., 2020). Allopurinol is an XO inhibitor (XOI), prescribed as the current first-line therapy (Stewart et al., 2019). In certain cases, allopurinol is prescribed in combination with lesinurad, which targets URAT1 (Alghamdi et al., 2020). However, serious adverse reactions of these drugs have been documented, namely skin rashes, aplastic anemia, renal insufficiency (Stewart et al., 2019), liver necrosis, hepatotoxicity (Ismail et al., 2019), allopurinol hypersensitivity syndrome and Stevens-Johnson syndrome (Strilchuk et al., 2019). On the other hand, the use of non-steroidal anti-inflammatory drugs (NSAIDs), colchicine, or corticosteroids to treat symptoms of gout attacks often causes abdominal pain (Lin et al., 2018; Wu et al., 2019), and gastrointestinal bleeding (Tseuguem et al., 2019). Adverse events following the drug intake are responsible for the low level of treatment compliance and unexpected increase in the burden of treatment costs.

The fruit of *Limonia acidissima* L. (*Rutaceae*) has been reported to contain potent antioxidants (Ko and Naing, 2020), antidiabetic and antibacterial properties (Srivastava et al., 2019). Phytochemical studies revealed the presence of alkaloids, flavonoids, phenols, terpenoids, tannins, fats, sterols, saponins, glycosides (Bagul et al., 2019; Lamani et al., 2021), stigmasterols, citric acid, alkaloids, coumarins, fatty acids, scoparone, xanthotoxin, sitosterol, steroids, alkaloids (Gharbieh et al., 2018; Srinivasan et al., 2015; Vijayvargia and Vijayvergia, 2014), coumarin (Salehi et al., 2020) and β-carotene (Rakhunde et al., 2014). However, information about the activity of this plant as an anti-hyperuricemia and anti-gout mechanism has not been widely reported.

It has been proven that serum urate balance is influenced by proteins related to renal urate transport that facilitate renal urate excretion, including urate transporter 1 (URAT1) and glucose transporter 9 (GLUT9) regulate renal uric acid reabsorption, while organic anion transporter 1 (OAT1) and native ATP-binding cassette subfamily G member 2 (ABCG2) regulate renal urate secretion (Wang et al., 2016). Elevated serum urate levels lead to kidney inflammation and down-regulation of renal organic ion transporters. Although the mechanism of kidney injury due to hyperuricemia is still poorly understood, it is believed that uric acid metabolism is closely related to the formation of free radicals. The accumulation of active oxygen generated during the restoration of uric acid metabolism is the precise mechanism leading to tissue damage due to oxidative stress (Huang et al., 2021).

Hyperuricemia and gout are closely related to metabolic diseases such as type 2 diabetes, which are facilitated by the protein Peroxisome Proliferator-Activated Receptor-γ (PPAR-γ). PPAR-γ is known as a transcription factor that regulates the expression of protein genes involved in glucose and lipid metabolisms (Ahmed and Lappin, 2018), decreases the inflammatory response through inhibition of the transcription factor of Nuclear Factor *kappa* B (NF-κB) (Meng et al., 2019), and regulates hyperuricemic activity (Wang et al., 2020). Previously, fatty acids have been suggested to be efficacious in regulating lipid homeostasis through the direct induction of PPAR-γ protein (Palomer et al., 2018). Oleic acid, an unsaturated fatty acid, has been reported to act as a PPAR-γ protagonist in overcoming insulin resistance in steotic cells (Palomer et al., 2018).

Although PPAR-γ protein is not the main target of anti-hyperuricemia and anti-gout mechanisms, a pre-

vious report suggested that unsaturated fatty acids reduced serum UA by inducing PPAR-γ protein activity (Suyanto et al., 2022). Herein, we aimed to create a network between the main fatty acids contained in the fruit of *L. acidissima* with their target receptors (PPAR-γ and Fatty Acid Binding Protein 3, FABP3) and their role as anti-hyperuricemia and anti-inflammatory on acute hyperuricemia and gouty arthritis in rats. Published literature has suggested the use of *in silico* methods to predictively elucidate the mode of actions of newly developed drugs, including those from natural products (Andalia et al., 2022; Purnama et al., 2021; 2022). Animal study to assess the effect of *L. acidissima* ethanolic extract on the protein expression of urate transporters (OAT1 and OAT3), which participate in facilitating the excretion of excess serum uric acid through the renal system. The effect on gout was studied by measuring the ankle joint edema of rats given an ethanolic fruit extract of *L. acidissima*.

## MATERIAL AND METHODS

### Chemicals

Materials used in this study include ethanol extract from *L. acidissima* (Aceh, Indonesia), potassium oxonate (PO), monosodium urate (MSU), ethanol 96%, dimethyl sulfoxide (DMSO), and carboxyl methyl cellulose (CMC) from Sigma-Aldrich (Selangor, Malaysia). Other chemicals used included ether ketamine, xylazine, formalin, sodium chloride (NaCl) 0.9%, and indomethacin from Kalbe Farma (Jakarta, Indonesia). Equipment and kits used in this study included Gas Chromatography-Mass Spectrometry (GC-MS QP2020 NX, Shimadzu, Kyoto, Japan), Quick-RNATM MiniPrep Plus (Zymo Research), cDNA was synthesized using ReverTra AceTM qPCR RT Master Mix with kit synthesis cDNA gDNA Remover (Toyobo), Applied Biosystem 7500 v.2.0.6 (Thermo Fisher Scientific, Selangor, Malaysia), ELISA Kit for tumor necrosis factor-*alpha* (TNFα) with "Cloud Clone Corp " brand (USA) with a product number of SEA133Ra, and micropipette (Eppendorf)

### Extraction and component identification

*L. acidissima* fruit was collected from the Aceh Besar area (5°29'11.3″N 95°25'40.3″E), which was peeled and separated from the seeds. The extraction was carried out at the Pharmacology Laboratory, Faculty of Veterinary Medicine, Universitas Syiah Kuala. The dried powder of *L. acidissima* fruit flesh (500 g) was macerated in a sealed container with 2.5 L of 96% ethanol for 72 h at room temperature (25 ± 1°C), and the cycle was renewed every 24 h (3 cycles in total). The filtrate was collected and treated in a rotary evaporator (40°C, 30 rpm) until all the solvent evaporated. The extract was sealed in a dark container until further use. Phytoconstituents of the extract were identified using gas chromatography-mass spectrometry (GC-MS QP2020 NX, Shimadzu, Kyoto, Japan). The GC-MS conditions used in this present study include column oven temperature 45°C, injection temperature 280°C, pressure 51.5 kPa, total flow 14 mL/min, column flow 1 mL/min, linear velocity 36.2 cm/s. The mass spectra for each separated compound were compared with the data from the NIST library. After the identification, the structure was downloaded in simplified molecular-input line-entry system (SMILE) format obtained from the PubChem database (http://www.pubchem.ncbi.nlm.nih.gov).

### Evaluation of absorption, distribution, metabolism, excretion, and toxicity profiles *in silico*

Absorption, distribution, metabolism, and excretion (ADME) pharmacokinetic properties of *L. acidissima* fruit extract were predicted on Swissadme (http://www.swissadme.ch). The pharmacokinetic properties of the compounds were judged based on Lipinski's rules of five following the predictions on SCFBIO (Supercomputing Facility for Bioinformatics and Computational Biology) (http://www.scfbio-iitd.res.in/software/drugdesign/lipinski.jsp). Meanwhile, the toxicity and median lethal dose ($LD_{50}$) were predicted by ProTox (https://tox-new.charite.de/protox_II/). The reference compound used was N-benzyl-1-[(4-chloro 3 fluorophenyl) methyl]-1H-indole-5-carboxamide.

### Network analysis

Possible protein targets of the compounds from *L. acidissima* fruit extract were predicted on the SEA Target database (Similarity ensemble approach) (https://www.sea.bkslab.org/). The minimum cut-off used was 0.5. The protein targets obtained were subsequently inputted into the STRING DB V.11.5 database (https://www.string-db.org/) with a medium confidence score of 0.4 for the *Homo sapiens* organism. It was followed by an analysis of Cytoscape version 3.8.2 to determine the role of proteins in the pathway. The GOlorize plug-in and Network Analysis on CytoScape were used in this study. GOlorize was used to determine the role of genes/proteins in the pathway using the BinGO (Gene Ontology) approach and visualized with a certain color. For BinGO-GOlorize, the statistical analysis was based on the Hypergeometric Test with Multiple Testing Correction from the Benjamini-Hochberg parameters, corrected with False Discovery Rate (FDR) correction, where $p<0.05$ was considered statistically significant.

## Molecular docking

*Preparation of ligands and receptors*

Compounds with the highest potential from previous in-silico analyses were proceeded to molecular docking. The 3D structure of each compound was constructed using MOE software (developed by Chemical Computing Group, Inc., Montreal, Canada) based on SMILES from the PubChem database(https://www.pubchem.ncbi.nlm.nih.gov/). The 3D structures of PPAR-γ (pdb id. 5TWO) and FABP3 (pdb id. 3WBG) proteins were used as receptors. All molecules were optimized based on the hydrogen atoms, partial energy, and energy. N-benzyl-1-[(4-chloro-3-flurophenyl)methyl]-1H-indole-5-carboxamide for PPAR-γ and 8-anilino-1-napthalene sulfonate for FABP3 were used as native ligands.

*Running molecular docking*

The docking process was carried out using the MOE application, starting with the validation of the VSP-51 docking integrated with the PPAR-γ receptor (pdb id. 5TWO) and the native ligand 1-anilinonaphthalene-8-sulphonic acid, which was integrated with the FABP3 (3WBG) receptor. Docking validation aimed to ensure that the docking results would have the same pose conformation as the experimental results, indicated by the RMSD (Root Means Square Deviation) value of less than 2. Thereafter, docking was carried out on all previously selected ligands. The docking results were expressed as free energy (ΔG) tabulated in a table and visualized through LigPlot (Hambal et al., 2022; Tallei et al., 2021).

## Effect of ethanolic extract of *L. acidissima* on organic anion transporter (OAT1 and OAT3) expression in kidneys of hyperuricemic rats

As reported in our previous papers (Yusnaini et al., 2023), the *in vivo* test was carried out using the ethanol extract of *L. acidissima* against male *Rattus norvegicus* strain Wistar (n = 30) obtained from the Animal Model Laboratory, Center for Biomedical Research, ResearchHub-Indonesia. These animals had characteristics of 12-14 weeks of age and a body weight (BW) between 200-300 g. All animals underwent an acclimatization period (7 days) to a light-dark cycle at 22 ± 2°C and were given food (protein content: 17%) *ad libitum*. Animals were divided into 6 groups (normal, hyperuricemia, allopurinol, and three groups of ethanol extract), each group consisting of 6 rats. All rats were fasted for 6 h before treatment. The normal group was injected intraperitoneally with saline (0.9% NaCl) for placebo control, while the other group was injected intraperitoneally with potassium oxonate 250 mg/kg BW (suspended in 0.9% NaCl).

Blood samples from each previously anesthetized rat, using ketamine (100 mg/kg BW) and xylazine (20 mg/kg BW) from Kalbe Farma (Indonesia), were taken from the abdominal aortic lateral tail vein. Blood samples were collected after 1 h of allopurinol or extract administration. In the allopurinol group, hyperuricemia-induced rats were treated with a dose of 10 mg/kg BW in 0.5% CMC suspension (10 mL) using a nasogastric tube. As for the extract group, each group was given a dose of 100, 200, and 400 mg/kg BW of *L. acidissima* ethanol extract in 0.5% (10 mL) CMC. The treatment (allopurinol or *L. acidissima* fruit extract) at 1 h intervals after PO induced was carried out every day for three consecutive days. Abdominal aortic blood was collected from each rat after 1 h after the last treatment. Then, rats were euthanized using ketamine (100 mg/kg) and xylazine (20 mg/kg), and internal organs were dissected. Ethical clearance for this study was previously granted by the ethics committee of the Faculty of Veterinary Medicine, Syiah Kuala University (No. 83/KEPH/XII/2020). Rats were excluded if they were seriously ill or injured and experienced significant weight loss (approximately 200 g) during the experiment.

## Determination of OAT1 and OAT3 gene expression

OAT1 and OAT3 gene expression was determined by qualitative polymerase chain reaction (PCR). RNA from rat kidneys was isolated using Quick-RNATM MiniPrep Plus (Zymo Research). cDNA was synthesized using ReverTra AceTM qPCR RT Master Mix with gDNA Remover cDNA synthesis kit (Toyobo). Reverse and forward sequences of DNA primers for each molecule measured using qualitative PCR have been presented in Table 1. Primers were designed based on previous literature indexed by the National Center for Biotechnology Information (NCBI, https://www.ncbi.nlm.nih.gov/nuccore/). Predenaturation was carried out at 95°C for 1 min before continuing with two other cycles: (1) performed at 95°C for 3 s with 40 repetitions and (2) at 60°C for 20 s. Cycle threshold (Ct) was taken for semi-quantification of mRNA amounts using Applied Biosystem 7500 v.2.0.6 (Thermo Fisher Scientific, Selangor, Malaysia). Gene expression was derived from $2^{-[Ct(OAT1\ and\ OAT3)-Ct(\beta\text{-actin})]}$, where normalization was based on endogenous β-actin. In this experiment, three replicates were made.

## Induction of gouty arthritis with monosodium urate (MSU) crystals

Adult male *Rattus norvegicus* (n = 30) were divided into 6 groups (normal, gouty arthritis, indomethacin,

**Table 1**. Primers were used to determine the expressions of OAT1 and OAT3 using qualitative PCR.

| Molecule | Sequence | PCR product size (bp) | NCBI reference sequence |
|---|---|---|---|
| β-actin | F: 5'-CCTAAGGCCAACCGTGAAAAGATG-3'<br>R: 5'-GTCCCGGCCAGCCAGGTCCAG-3' | 219 | NM_007393.3 |
| OAT1 | F: 5'- CTTTCCCGCACAATGGCACAGAGG-3'<br>R: 5'- GTCCGCCAGGTAGCCAAACATCAT-3' | 209 | NM_008766.3 |
| OAT3 | F: 5'- CCAAACGCCAGTCTTCCCAATGA-3'<br>R: 5'- TGCGGCCAAACCTGTCTGA-3' | 211 | NM_031194.5 |

F: Forward; R: Reverse

and three groups of ethanol extract), each group consisting of 6 rats each: (1) The normal group was injected with saline (0.9% NaCl) for placebo control; (2) gouty arthritis model with MSU crystal injection (MSU + vehicle); (3) the indomethacin treated group (MSU + indomethacin 10 mg/kg, p.o.); (4) ethanolic extract of *L. acidissima* (EEL) 100 mg/kg; (5) EEL 200 mg/kg; and (6) EEL 400 mg/kg. This experimental procedure was adopted and modified from Tseuguem et al. (2019). Monosodium urate crystals were suspended in 0.9% sterile saline immediately before use. Briefly, on the first day, the rats were anesthetized with ether after the right ankle skin was sterilized with 75% ethanol. Then, 0.05 mL (4 mg) of monosodium urate suspension (MSU) was injected into the right ankle, precisely into the articular cavity in the gap between the tibiofibular and tarsal bones to induce gout in all groups except the normal group.

Treatment was carried out intragastric (oral) according to the group. Vehicle, indomethacin, and EEL were given every day for 3 days at the same time. Joint inflammation was assessed by measuring the thickness of the ankle (in millimeters) using an vernier caliper at 0, 4, 12, 24, 48, and 72 h after the first MSU injection. At the end of the experimental period (72 h), all rats were euthanized with ketamine (100 mg/kg) and xylazine (20 mg/kg). Blood samples were collected from eye socket veins 24 h after injection of MSU crystals and centrifuged at 3000 rpm for 10 min at 4°C, and serum was collected and stored at −80 °C until further testing.

### Statistical analysis

Data obtained in this study were processed statistically in GraphPad PRISM version 9 (GraphPad Software, San Diego, CA, USA). The normality test was based on the Shapiro-Wilk test (α = 0.05). Normally distributed data were analyzed for statistical differences based on paired *t*-tests. Otherwise, the statistical difference was observed based on the *p*-value obtained from the Wilcoxon test.

## RESULTS

### GC-MS analysis of *L. acidissima* fruit extract

Identification of plant active compounds could be carried out using various methods, starting with phytochemical tests to observe what groups of active compounds are contained in the plant, to using the "near-infrared spectroscopy" (NIRS) technique, which is able to quickly classify the quality of active compounds (Ikhsan et al., 2021; Yusnaini et al., 2021). However, the use of GC-MS is still in great demand because of its high resolution, specificity, and sensitivity. Its operation is flexible as it can be easily combined with other physical or chemical instruments. Moreover, the technique could provide structural information with only a small amount of sample and in a relatively short operating time, hence the efficiency. Results from GC-MS analysis on *L. acidissima* fruit extracts obtained using n-hexane, ethyl acetate, ethanol and methanol as solvents, respectively, have been presented in Table 2 and Supplement 1. The MS spectral data were compared and matched with those from the National Institute of Standards and Technology (NIST) compound library.

### Data on "SMILE" of *L. acidissima* fruit flesh extract compounds

The dominant compounds of the *L. acidissima* fruit extracts, as identified by GC-MS, were determined for their ID code and SMILE (simplified molecular-input line-entry system) based on the PubChem database. The data from this analysis have been presented in Table 3. The reference compound used was N-benzyl-1-[(4-chloro-3-fluorophenyl)methyl]-1H-indole-5-carboxamide.

### Evaluation of the pharmacokinetic properties of ligands

The absorption, distribution, metabolism, excretion, and toxicity (ADMET) properties of each ligand were evaluated. The ligand activity in the body and

**Table 2.** Dominant compounds of *n*-hexane, ethyl acetate, ethanol, and methanol content of *L. acidissima* fruit extract.

| Extract | Peak | RT (min) | Concentration (%) | SI (%) | Name |
|---|---|---|---|---|---|
| ***n*-Hexane** | | | | | |
| | 12 | 17.549 | 5.8 | 95 | 1-Heptadecene |
| | 17 | 19.234 | 1.3 | 96 | Palmitoleic acid |
| | 18 | 19.459 | 20.4 | 96 | n-Hexadecanoic acid |
| | 22 | 21.281 | 26.6 | 93 | Oleic acid |
| | 23 | 21.472 | 5.8 | 92 | Octadecanoic acid |
| **Ethyl acetate** | | | | | |
| | 12 | 19.250 | 1.1 | 96 | Palmitoleic acid |
| | 13 | 19.480 | 19.2 | 96 | n-Hexadecanoic acid |
| | 17 | 20.843 | 5 | 91 | 9-Octadecenoic acid (Z)-, methyl ester |
| | 19 | 21.306 | 28.7 | 93 | Oleic acid |
| | 20 | 21.479 | 4.9 | 94 | Octadecanoic acid |
| | 23 | 23.852 | 2.66 | 81 | Ergost-5-en-3-ol, (3*beta*.)- |
| | 25 | 24.572 | 4.2 | 93 | Stigmasterol |
| | 27 | 26.013 | 7.6 | 91 | *gamma*-Sitosterol |
| | 31 | 28.286 | 0.6 | 86 | Lupeol |
| **Ethanol** | | | | | |
| | 2 | 4.090 | 6.5 | 95 | 2-Pentanone,4-hydroxy-4-methyl- |
| | 4 | 19.454 | 3.2 | 96 | n-Hexadecanoic acid |
| | 6 | 21.264 | 4.4 | 95 | Oleic acid |
| | 8 | 23.871 | 11.6 | 90 | Ergost-5-en-3-ol(3*beta*.)- |
| | 9 | 24.584 | 13.4 | 92 | Stigmasterol |
| | 10 | 26.029 | 27.6 | 93 | *gamma*-Sitosterol |
| **Methanol** | | | | | |
| | 2 | 4.126 | 14.9 | 96 | 2-Pentanone,4-hydroxy-4-methyl- |
| | 5 | 19.464 | 7.3 | 96 | n-Hexadecanoic acid |
| | 7 | 20.854 | 12.6 | 91 | 9-Octadecenoic acid (Z)-, methyl ester |
| | 9 | 21.272 | 14.3 | 95 | Oleic acid |
| | 10 | 21.492 | 3 | 85 | Octadecanoic acid |

RT: Retention time; SI: Similarity index.

its potential as an active compound candidate were tested based on Lipinski's rule of five. Toxicity classification refers to the globally harmonized system (GHS) of classification and labeling of chemicals. Data from the foregoing analyses have been presented in Table 4. Of the compounds predicted, 11 fulfill the Lipinski's rule of five (Lipinski, 2004). Toxicity results using the Protox-II, based on the $LD_{50}$ (mg/kg), suggested the compound to be categorized in toxicity class 4 to 6. This indicates that the compounds identified in *L. acidissima* fruit extract, in this present study, are safe for consumption.

## Network analysis

The target protein that can interact with the bioactive content of *L. acidissima* that meets Lipinski's rule of five was predicted by the SEA Target approach. The best score validation was based on the Tanimoto Coefficient Similarity (MaxTC) score parameter with a cut-off of 0.5 and a maximum score of 1. The data from this analysis have been presented in Table 5 and Fig. 1. The best score was shown by oleic acid, n-hexadecanoic acid, and palmitoleic acid compounds by targeting PPAR-γ and FABP3. These interactions were predicted to facilitate the regulation of XO.

**Table 3.** ID code for the "smiles" format of the *L. acidissima* fruit extract compound.

| Molecule | PubChem ID | SMILE | Formula |
|---|---|---|---|
| Oleic acid | 445639 | CCCCCCCCC=CCCCCCCCC(=O)O | $C_{18}H_{34}O_2$ |
| n-Hexadecanoic acid | 985 | CCCCCCCCCCCCCCCC(=O)O | $C_{16}H_{32}O_2$ |
| Octadecanoic acid | 5281 | CCCCCCCCCCCCCCCCCC(=O)O | $C_{18}H_{36}O_2$ |
| 1-Heptadecene | 23217 | CCCCCCCCCCCCCCCC=C | $C_{17}H_{34}$ |
| *gamma*-Sitosterol | 457801 | CCC(CCC(C)C1CCC2C1(CCC3C2CC=C4C3(CCC(C4)O)C)C)C(C)C | $C_{29}H_{50}O$ |
| Stigmasterol | 5280794 | CCC(C=CC(C)C1CCC2C1(CCC3C2CC=C4C3(CCC(C4)O)C)C)C(C)C | $C_{29}H_{48}O$ |
| Ergost-5-en-3-ol, (3.*beta*.)- | 6428659 | CC(C)C(C)CCC(C)C1CCC2C1(CCC3C2CC=C4C3(CCC(C4)O)C)C | $C_{28}H_{48}O$ |
| Tris(2,4-di-tert-butylphenyl) phosphate | 14572930 | CC(C)(C)C1=CC(=C(C=C1)OP(=O)(OC2=C(C=C(C=C2)C(C)(C)C)C(C)(C)C)OC3=C(C=C(C=C3)C(C)(C)C)C(C)(C)C)C(C)(C)C | $C_{42}H_{63}O_4P$ |
| 2-Pentanone,4-hydroxy-4-methyl- | 618244 | CC(C)(CC(=O)C(C1=CC=CC=C1)(C2=CC=CC=C2)C3=CC=CC=C3)O | $C_{24}H_{24}O_2$ |
| 9-Octadecenoic acid (Z)-, methyl ester | 5364509 | CCCCCCCCC=CCCCCCCCC(=O)OC | $C_{19}H_{36}O_2$ |
| Palmitolic acid | 445638 | CCCCCCC=CCCCCCCCC(=O)O | $C_{16}H_{30}O_2$ |
| Lupeol | 259846 | CC(=C)C1CCC2(C1C3CCC4C5(CCC(C(C5CCC4(C3(CC2)C)C)(C)C)O)C)C | $C_{30}H_{50}O$ |
| N-benzyl-1-[(4-chloro-3-fluorophenyl)methyl]-1H-indole-5-carboxamide (native ligand) | 124081193 | c1ccc(cc1)CNC(=O)c2ccc3c(c2)ccn3Cc4ccc(c(c4)F)Cl | $C_{23}H_{18}Cl\ FN_2O$ |

SMILE: Simplified molecular-input line-entry system, a specification in line notation to describe the structure of a chemical species using short ASCII strings.

**Table 4.** Absorption, distribution, metabolism, excretion, and toxicity (ADMET) content of *L. acidissima* fruit extract.

| Molecule | MW (g/mol) <500 Da | Rota table bonds ≤10 | HBA ≤10 | HBD ≤5 | MR | Consensus Log P ≤5 | Lipinski ≤1 | GI abs | Predicted $LD_{50}$ (mg/kg) | Predicted toxicity class |
|---|---|---|---|---|---|---|---|---|---|---|
| Oleic acid | 282.46 | 15 | 2 | 1 | 89.94 | 5.71 | Yes | High | 480 | 4 |
| n-Hexadecanoic acid | 256.42 | 14 | 2 | 1 | 80.80 | 5.20 | Yes | High | 900 | 4 |
| Octadecanoic acid | 284.48 | 16 | 2 | 1 | 90.41 | 5.93 | Yes | High | 900 | 4 |
| 1-Heptadecene | 238.45 | 14 | 0 | 0 | 83.36 | 6.82 | Yes | Low | 5050 | 6 |
| *gamma*-Sitosterol | 414.71 | 6 | 1 | 1 | 133.23 | 7.19 | Yes | Low | 890 | 4 |
| Stigmasterol | 412.69 | 5 | 1 | 1 | 132.75 | 6.97 | Yes | Low | 890 | 4 |
| Ergost-5-en-3-ol,(3.*beta*)- | 400.68 | 5 | 1 | 1 | 128.42 | 6.90 | Yes | Low | 890 | 4 |
| 2-Pentanone,4-hydroxy-4-methyl- | 344.45 | 6 | 2 | 1 | 105.70 | 4.50 | Yes | High | 1250 | 4 |
| 9-Octadecenoic acid (Z)-, methyl ester | 296.49 | 16 | 2 | 0 | 94.26 | 5.95 | Yes | High | 3000 | 5 |
| Palmitoleic acid | 254.41 | 13 | 2 | 1 | 80.32 | 4.92 | Yes | High | 1190 | 4 |
| Lupeol | 426.72 | 1 | 1 | 1 | 135.14 | 7.26 | Yes | Low | 2000 | 4 |
| N-benzyl-1-[(4-chloro 3 fluorophenyl)methyl]-1H-indole-5-carboxamide (native ligand) | 493.85 | 6 | 2 | 1 | 110.14 | 4.88 | Yes | High | 583 | 4 |

MW: Molecular Weight (g/mol); HBA: Hydrogen Bond Acceptor; HBD: Hydrogen Bond Donor; MR: Molar refractivity; LogP: Lipophilicity; $LD_{50}$: Median Lethality Dose; GI abs: Gastrointestinal absorption.

**Table 5.** Prediction of SEA target proteins from *L. acidissima.*

| Compound | Target key | Target molecule | Description | *P*-value | MaxTC |
|---|---|---|---|---|---|
| Oleic acid | PPARG_HUMAN | PPARG | Peroxisome proliferator-activated receptor *gamma* | $5.19E^{-10}$ | 1 |
| | FABPH_HUMAN | FABP3 | Fatty acid-binding protein, heart | $1.20E^{-26}$ | 1 |
| | S22A6_HUMAN | SLC22A6 | Solute carrier family 22 member 6 | $3.07E^{-17}$ | 0.74 |
| n-Hexadecanoic acid | S22A6_HUMAN | SLC22A6 | Solute carrier family 22 member 6 | $5.84E^{-23}$ | 1 |
| | S22A8_HUMAN | SLC22A8 | Solute carrier family 22 member 8 | $9.77E^{-19}$ | 1 |
| | FABPH_HUMAN | FABP3 | Fatty acid-binding protein, heart | $1.46E^{-22}$ | 0.74 |
| Palmitoleic acid | FABPH_HUMAN | FABP3 | Fatty acid-binding protein, heart | $1.20E^{-26}$ | 1 |
| | PPARG_HUMAN | PPARG | Peroxisome proliferator-activated receptor *gamma* | $5.19E^{-10}$ | 1 |
| | S22A6_HUMAN | SLC22A6 | Solute carrier family 22 member 6 | $3.07E^{-17}$ | 0.74 |
| | S22A8_HUMAN | SLC22A8 | Solute carrier family 22 member 8 | $4.87E^{-14}$ | 0.74 |

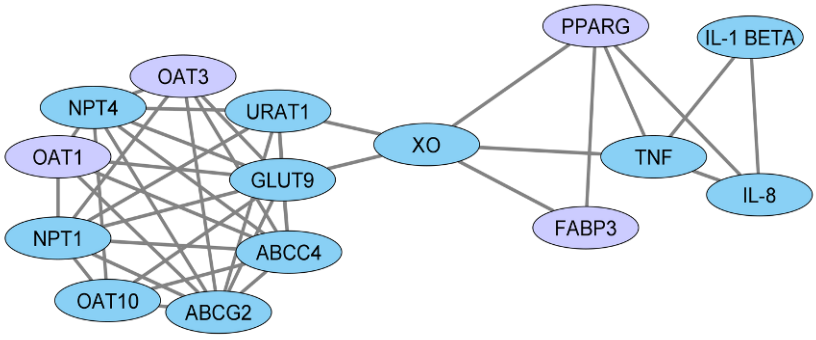


**Figure 1**. Visualization of the interaction of the target protein of *L. acidissima* (purple) with the proteins involved in hyperuricemia and gout (blue).

Oleic acid, n-hexadecanoic acid, and palmitoleic acid were also predicted to target OAT1 and OAT3, both of which were associated with UA excretion.

PPAR-γ and FABP3 are revealed to be connected without XO mediation. Therefore, oleic acid and palmitoleic acid compounds are predicted to be able to influence XO function through direct modulation of PPAR-γ and FABP3. Meanwhile, in targeting URAT1, OAT1, and OAT3, oleic acid and palmitoleic acid compounds require protein intermediaries, including nicotinate phosphoribosyl transferase (NPT)1, NPT4, GLUT9, ATP ABCC4, and others (Fig. 1).

In this study, a networking analysis of the target protein and protein of interest for the bioactive compound *L. acidissima* involved in hyperuricemia and gout was also carried out (Fig. 2). Analysis using Cytoscape version 3.8.2 was carried out to determine the role of proteins in the pathway. The nodes represent the total number of bioactives, target proteins, and signaling pathways, indicating that the pathways interact with therapeutic abilities against hyperuricemia and gout. XO is the most significant target protein among other protein-associated pathways that are directly linked to signaling pathways.

The pathway analysis obtained from STRING was then processed with GOlorize on CytoScape with the BinGO (Gene Ontology) approach to determine the role of proteins in the pathway. The results of the analysis showed that the target compounds (oleic acid, n-hexadecanoic acid, and palmitoleic acid) could interact with the protein of interest, namely URAT1(SLC22A12) along with proinflammatory factors—TNF and IL-8 (CXCL8) (Table 6).

Likewise, based on networking analysis in Cytoscape, XO has been revealed to have the highest value of Betweenness Centrality. Therefore, the enzyme has a significant role in the concerned pathway (Fig. 2). In addition, n-hexadecanoic acid and palmitoleic acid were also found to target OAT1 (SLC22A6) and OAT3 (SLC22A8). Compounds in *L. acidissima* could also target Peroxisome Proliferator Activated Receptor *Gamma* (PPARG) and Fatty Acid Binding Protein 3

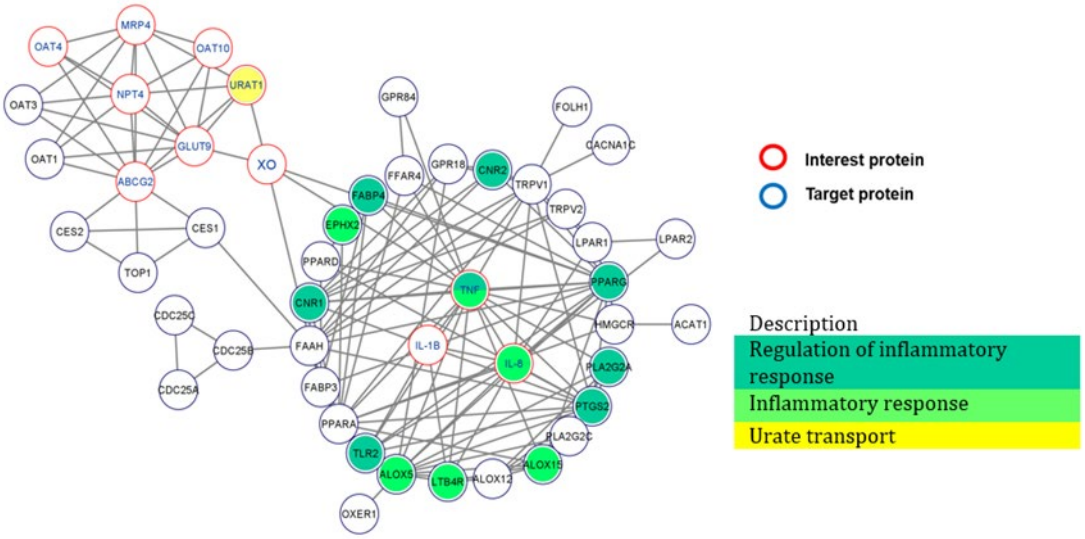


**Figure 2.** Visualization of interactions of target proteins of *L. acidissima* with proteins playing a role in hyperuricemia and inflammation (gout).

**Table 6.** Analysis of Gene Ontology results with GOlorize in Cytoscape.

| GO-ID | p-value | corr p-value | Description | Genes in test set |
|---|---|---|---|---|
| 50727 | $4.61E^{-10}$ | $1.89E^{-07}$ | Regulation of inflammatory response | FABP4; CNR2; CNR1; PLA2G2A; PPARG; PTGS2; TNF; TLR2 |
| 15747 | $3.29E^{-03}$ | $1.84E^{-02}$ | Urate transport | SLC22A12 (URAT1) |
| 6954 | $5.46E^{-04}$ | $5.70E^{-03}$ | Inflammatory response | CXCL8; ALOX5\|; EPHX2; ALOX15; TNF; LTB4R |

**Table 7.** Ligand docking results against PPAR-γ and FABP3 receptors.

| Compound | PPAR-γ | | FABP3 | |
|---|---|---|---|---|
| | Affinity (kcal/mol) | H-bound | Affinity (kcal/mol) | H-bound |
| Palmitoleic acid | -11.28 | Glu 343 | -12.31 | Arg 106 (2×), Thr 40 |
| Oleic acid | -12.54 | Leu 228 | -13.09 | Arg 106 (2×), Thr 40 |
| Octadecanoic acid | -11.76 | Tyr 327 | -11.38 | Arg 106 (2×), Thr 40 |
| n-Hexadecanoic acid | -11.40 | Ile 326 | -10.55 | Arg 106 (2×), Thr 40 |
| N-benzyl-1-[(4-chloro-3-fluorophenyl)methyl]-1H-indole-5-carboxamide (native ligand control) | -9.92 | Ser 289, Tyr 327 | | |
| 8-Anilino-1-napthalene sulfonate (native ligand control) | | | -10.31 | Arg 126 |

(FABP3) which facilitate the interaction between the compounds and XO.

## Molecular docking

Molecular docking was performed specifically by targeting a protein binding site that bound to PPAR-γ and FABP3 agonists. The validation results of docking native ligands for PPAR-γ and FABP3 receptors showed RMSD values of 1.40 Å and 1.03 Å, respectively. The docked fatty acids were selected based on the most dominant peak from the GC-MS results (as presented in Table 2). Values of affinity and hydrogen bonding are presented in Table 7, while the visualization of the molecular docking has been presented in Fig. 3.

Docking studies for PPAR-γ and FABP3 showed a better affinity for all ligands than controls. Oleic acid showed the best interaction stability with PPAR-γ and FABP3 with affinity values of -11.28 kcal/mol and -13.09 kcal/mol, respectively. While the control

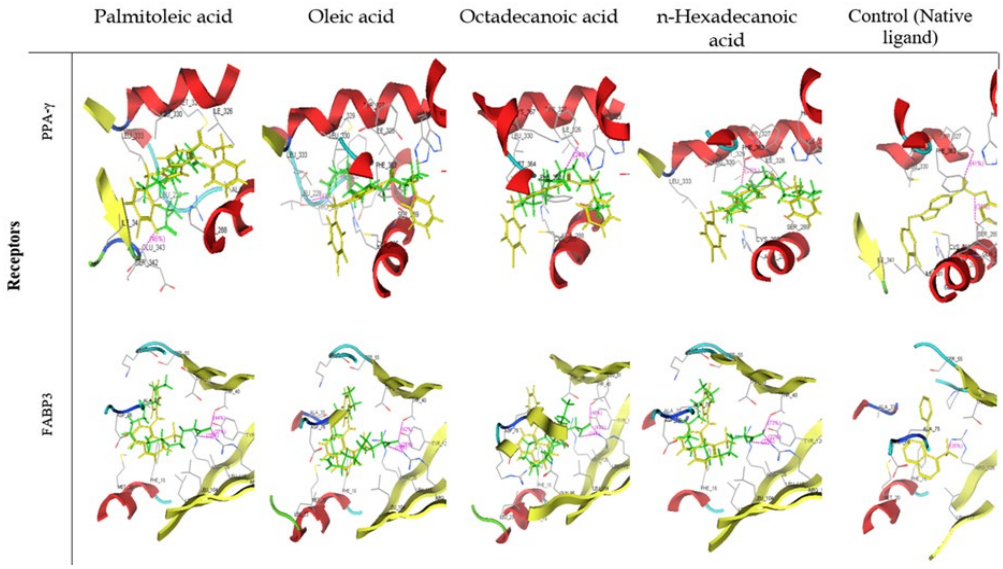


**Figure 3.** 2D and 3D visualization of ligand interaction models with PPAR-γ and FABP3.

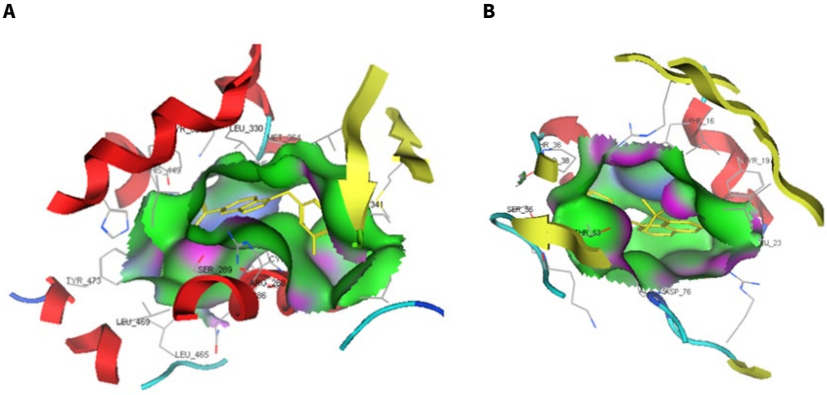


**Figure 4.** Binding site pocket of native ligands of **(A)** PPAR-γ and **(B)** FABP3.

(PPAR-γ and FABP3) agonists had affinities of -9.92 kcal/mol and -10.31 kcal/mol, respectively. Oleic acid interacts with the PPAR-γ receptor to form hydrogen bonds with the amino acid Glu 343, while the PPAR-agonist ligands form hydrogen bonds with the amino acids Ser 289 and Tyr 327. Oleic acid also interacts with the FABP3 receptor to form hydrogen bonds with the amino acid Arg 106. (2×) and Thr 40, while the agonist FABP3 ligand formed hydrogen bonds with the amino acid Arg 126.

Although the test and control ligands form hydrogen bonds with different amino acids, they are still in the same binding site area, so they have an agonist function against the native ligands for the two receptors. The binding site area is dominated by green color (Fig. 4), which indicates a very dominant hydrophobic interaction compared to those colored in blue (Vander Wals bonds) and purple (hydrogen bonds). Hence, it is suspected that the interaction of the ligand to PPAR-γ and FABP3 is more dependent on hydrophobic bonds as compared to hydrogen bonds. PPAR-γ and FABP3 receptors have a narrow gap in the form of a "hydrophobic groove" as the main area of contact between the ligand and the receptor (Susanty et al., 2021). The fatty acids oleic acid, n-hexadecanoic acid, and palmitoleic acid are thought to be able to pass through the narrow gap and interact with the two receptors, thereby possessing better affinity as compared with native ligands.

## Expression profile of OAT1 and OAT3 in renal tissue

The lowest OAT1 expression has been shown in the hyperuricemia group (30.07 ± 1.95), and the highest has been seen in the 400 mg EEL group (35.76 ± 1.19). The lowest OAT3 expression was found in the hyperuricemia group (30.86 ± 1.59), and the highest was found in the allopurinol group (33.40 ± 1.44), and EEL 400 mg (33.41 ± 0.56) (Table 8). Allopurinol was the reference compound.

**Table 8**. Protein expression levels of OAT1 and OAT3 in renal tissue.

| Variable | Group | Mean ± SD | Median | Min-Max |
|---|---|---|---|---|
| OAT1 | Normal | 31.96 ± 2.60 | 30.32 | 29.57-34.80 |
| | Hyperuricemia | 30.07 ± 1.95 | 29.55 | 28.87-33.52 |
| | Allopurinol | 34.55 ± 1.42 | 34.33 | 32.39-35.85 |
| | EEL 100 mg | 32.74 ± 0.84 | 33.35 | 31.82-33.36 |
| | EEL 200 mg | 34.71 ± 1.56 | 35.85 | 32.99-35.55 |
| | EEL 400 mg | 35.76 ± 1.19 | 36.64 | 32.79-33.83 |
| OAT3 | Normal | 31.60 ± 1.86 | 30.97 | 29.13-33.47 |
| | Hyperuricemia | 30.86 ± 1.59 | 30.92 | 29.52-33.42 |
| | Allopurinol | 33.40 ± 1.44 | 33.41 | 31.04-34.57 |
| | EEL 100 mg | 31.05 ± 0.98 | 30.78 | 30.45-32.79 |
| | EEL 200 mg | 31.96 ± 0.81 | 32.55 | 31.07-32.55 |
| | EEL 400 mg | 33.41 ± 0.56 | 33.82 | 32.79-33.83 |

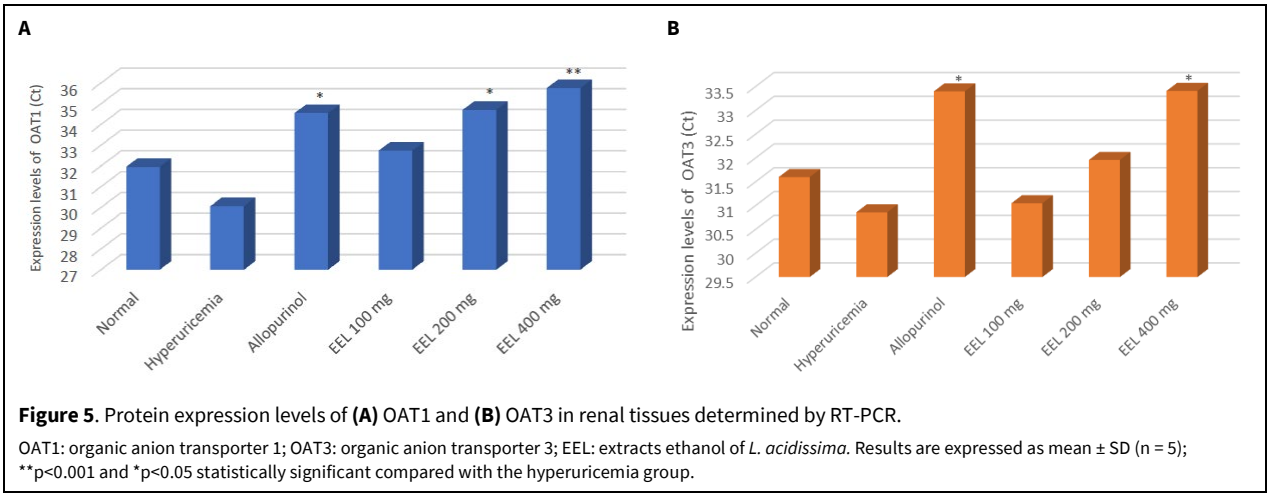


**Figure 5**. Protein expression levels of **(A)** OAT1 and **(B)** OAT3 in renal tissues determined by RT-PCR.

OAT1: organic anion transporter 1; OAT3: organic anion transporter 3; EEL: extracts ethanol of *L. acidissima*. Results are expressed as mean ± SD (n = 5); **p<0.001 and *p<0.05 statistically significant compared with the hyperuricemia group.

Based on the results of the post hoc one-way ANOVA statistical test, compared to the hyperuricemic group, there was a significant increase in OAT1 expression in the allopurinol (p = 0.004), EEL 200 mg (p = 0.003) and EEL 400 mg/kg group (p = 0.001). While the expression of OAT 3 significantly increased in the allopurinol and EEL 400 mg/kg groups (p = 0.048) in both groups (Fig. 5; Table 9).

## Monosodium urate crystal-induced inflammation in rats

The degree of edema was determined by assessing joint edema in the rat ankle (Table 10). MSU crystal-induced rat joint edema values significantly increased in the gouty arthritis model (MSU + vehicle) group at 4 to 48 h and began to decrease after 72 h. The joint edema of the indomethacin group and the intervention group with *L. acidissima* ethanol extract (EEL100, EEL200, and EEL400 mg/kg) also increased at 4 h, but after 48 h, the edema began to improve faster than the gouty arthritis group. Group of *L. acidissima* 400 mg/kg showed the most significant decrease in edema than the other groups (Fig. 6).

As shown in Fig. 6, MSU crystal injection showed an impact on ankle edema. Edema began to appear after 4 h and reached a maximum after 24 h, then gradually decreased. Edema reduction significantly occurs after 24 h in the EEL and indometacin groups compared to gouty arthritis (more than 72 h). EEL was able to inhibit edema and present inflammatory reduction activities (p<0.001).

**Table 9**. Effects of *L. acidissima* ethanolic extract and allopurinol on protein expression of OAT1 and OAT3 in renal tissues in hyperuricemia rats.

| Variable | Group | Mean ± SD | *p*-Value |
|---|---|---|---|
| OAT1 | Hyperuricemia | 30.07 ± 1.95 | |
| | Allopurinol | 34.55 ± 1.42 | **0.004*** |
| | EEL 100 mg | 32.74 ± 0.84 | 0.168 |
| | EEL 200 mg | 34.71 ± 1.56 | **0.003*** |
| | EEL 400 mg | 35.76 ± 1.19 | **<0.001**** |
| OAT3 | Hyperuricemia | 30.86 ± 1.59 | |
| | Allopurinol | 33.40 ± 1.44 | **0.048*** |
| | EEL 100 mg | 31.05 ± 0.98 | 1.000 |
| | EEL 200 mg | 31.96 ± 0.81 | 0.760 |
| | EEL 400 mg | 33.41 ± 0.56 | **0.048*** |

Statistically significant at **p<0.001 and *p<0.05 compared with the hyperuricemia group by post hoc one-way ANOVA analysis (n = 5).

**Table 10.** Changes in the thickness of joint edema of MSU crystal-induced rats.

| Time of measurement (h) | Ankle thickness (mm) in rats (mean ± SD) | | | | | |
|---|---|---|---|---|---|---|
| | Normal | Gouty arthritis | Indomethacin | EEL 100 mg | EEL 200 mg | EEL 400 mg |
| 0 | 4.50 ± 0.50 | 4.20 ± 0.27 | 4.80 ± 0.27 | 4.40 ± 0.54 | 4.70 ± 0.44 | 4.70 ± 0.44 |
| 4 | 4.50 ± 0.50 | 5.20 ± 0.44 | 5.50 ± 0.35 | 5.30 ± 0.67 | 5.70 ± 0.67 | 5.40 ± 0.22 |
| 12 | 4.50 ± 0.50 | 7.20 ± 0.27 | 6.90 ± 0.22 | 7.40 ± 0.41 | 6.80 ± 0.44 | 6.80 ± 0.44 |
| 24 | 4.50 ± 0.50 | 9.50 ± 0.35 | 7.90 ± 0.54 | 8.50 ± 0.50 | 8.00 ± 0.61 | 7.70 ± 0.67 |
| 48 | 4.50 ± 0.50 | 9.70 ± 0.44 | 6.80 ± 0.44 | 8.10 ± 0.65 | 6.70 ± 0.27 | 6.10 ± 0.74 |
| 72 | 4.50 ± 0.50 | 6.80 ± 3.81 | 5.64 ± 0.72 | 5.60 ± 3.18 | 5.40 ± 0.65 | 4.80 ± 0.27 |

Results are expressed as mean ± SD (n = 5). Statistically significant at **p<0.001 and *p<0.05 compared with the hyperuricemia group by post hoc one-way ANOVA analysis.

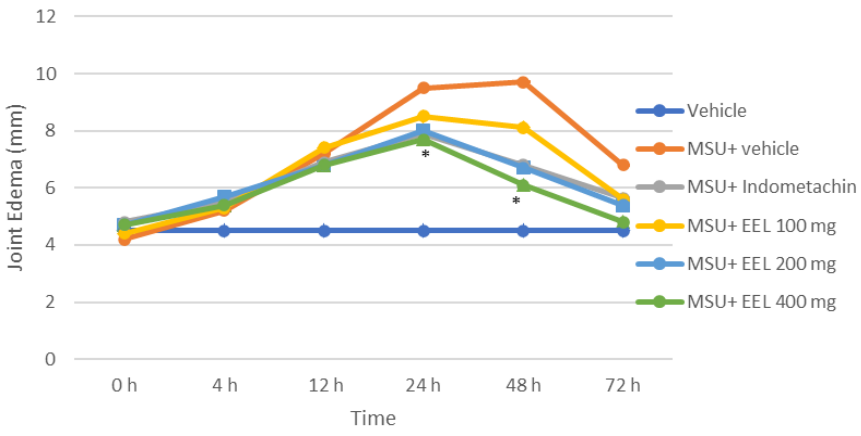


**Figure 6**. Effect of *L. acidissima* ethanolic extract on the ankle edema of MSU crystal-induced rats.

Results are expressed as mean ± SD (n = 5). Statistically significant at **p<0.001 and *p<0.05 compared with the hyperuricemia group by post hoc repeated ANOVA analysis.

## DISCUSSION

GC-MS analysis revealed the dominant presence of fatty acids, sterols such as γ-sitosterol, stigmasterol, ergost-5-en-3-ol, (3*beta*.), and ester groups. This is in line with previous research, which identified the majority of palmitic acid, stearic acid, oleic acid, linoleic, and linolenic acids in *L. acidissima* extract (Lamani et al., 2021). *n*-Hexadecanoic acid has been considered to have antioxidant and anti-inflammatory activities as well as an inhibiting activity against XO. Hyperuricemia is an independent risk factor for renal tissue damage (Andriana et al., 2019; Jenecius et al., 2012). The presence of oleic acid, n-hexadecanoic acid, palmitoleic acid, octadecanoic acid in *L. acidissima* fruit extract is expected to activate PPARγ receptors so that it can inhibit the inflammatory response concomitant to UA deposition-induced free radical formation. PPARγ may function as an unsaturated fatty acid sensor in controlling cellular oxidative stress and preventing cell apoptosis and kidney tissue necrosis, which are related to hyperuricemia.

In this study, there was an effect of increasing the expression of OAT1 and OAT3 as uric acid transporter in the kidneys to create hypouricemia. Upregulation of OAT1 and OAT 3 can lead to the action of uricosuric EEL in hyperuricemia rats. Uric acid serum levels are associated with purine metabolism and are influenced by kidneys purine excretion (Yong et al., 2018). The protein OAT1 and OAT3 expression in rat kidney tissue treated with allopurinol and EEL is higher than in the hyperuricemia model. These results support OAT1 and OAT3 as transporter secretions that are useful for facilitating uric acid excretion (Chen et al., 2016). The protein expression level in organs is closely related to the degree of organ damage. It has been reported that hyperuricemia causes massive amounts of tissue necrosis and ultimately downregulates the expression of all proteins. When an anti-hyperuricemic drug is used, it reduces kidney damage and protects kidney function, which then increases the expression of all proteins in the kidney. Therefore, it is most likely that the decrease in uric acid levels influences the increased protein expression in the kidney.

In the gouty animal model, injection of MSU crystals into the ankle joint cavity of rats stimulated an inflammatory response mediated by macrophages and neutrophils, thus triggering symptoms of acute gout. Significant ankle edema accompanied by an extensive inflammatory response is an important sign in determining the degree of inflammation. This edema indicates that neutrophils move toward the joint cavity and actively phagocytize MSU crystals, causing membrane lysis and releasing inflammatory cytokines and free radicals, amplifying the inflammatory response (Müller et al., 2019).

Previous studies reported that fatty acids and their derivatives have been shown to bind and activate PPARγ, a member of the nuclear receptor superfamily of ligand-inducible transcription factors. PPARγ is a receptor for dietary fats such as oleic, linoleic and linolenic acids. PPARγ is involved in binding and responding to various lipid metabolism, plays an important role in cell immunity (immune response) with various processes, ranging from production, maturation, activation and migration of cytokines and antigens (Ahmadian et al., 2013). PPARγ can increase the expression of various antioxidant genes and decrease the synthesis of pro-inflammatory mediators, so it is considered the most important regulator of the cellular response to oxidative stress (Muzio et al., 2021). Monounsaturated fatty acids such as oleic acid exhibit analgesic and anti-inflammatory activity by downregulating the expression of pro-inflammatory cytokines such as TNF-α, interleukin 6 (IL-6) and nitric oxide (NO), as well as the production of free radicals in macrophage-stimulated lipopolysaccharide cells. Meanwhile, polyunsaturated fatty acids could reduce pro-inflammatory mediators or downregulate inflammatory cytokines such as IL-6, TNF-α, and monocyte chemotactic protein-1 (MCP-1) (Libório et al., 2020).

Docking studies showed predominant fatty acids in *L. acidissima* (oleic acid, n-hexadecanoic acid, and palmitoleic acid) are predicted to have therapeutic effects against hyperuricemia and gout arthritis by mainly targeting PPAR-γ and FABP3. This is in line with a previous study reporting that fatty acids and their metabolites have been shown to bind and activate PPARγ (Ahmadian et al., 2013). Activation of PPAR-γ exerts an anti-inflammatory effect by inhibiting the nuclear factor *kappa* B (NF-κB) pathway and triggering antifibrosis (Wang et al., 2020). NF-κB in endothelial cells involved in the adhesion and transmigration of monocytes and lymphocytes by increasing the expression of cell adhesion molecules like ICAM-1 (intercellular adhesion molecule-1), VCAM-1 (vascular cell adhesion molecule-1) and E-selectin, regulating the production of inflammatory cytokines (TNFα, IL-6, and IL-8) and promote apoptosis (de Souza et al., 2018).

## CONCLUSION

The results of this study revealed that the *n*-hexane, ethyl acetate, ethanol, and methanol extracts of *L. acidissima* fruit predominantly consisted of fatty acid compounds, sterol groups, and terpenoids. The main fatty acid group in *L. acidissima* has the potential to modulate the activity of proteins involved in the

XO inhibitory pathway and uric acid excretion. Computational simulations of *in silico* docking also provide supportive evidence at the molecular level about the significant binding of fatty acids to XO. Oleic acid and palmitoleic acid compounds are predicted to be able to influence XO function through direct modulation of PPAR-γ and FABP3. Meanwhile, in influencing URAT1, oleic acid and palmitoleic acid compounds that target OAT1 and OAT3 affect URAT 1 through the mediation of NPT1, NPT4, GLUT9, ABCC4, ABCG2, and OAT 10 proteins. Ethanolic extract of *L. acidissima* has the potential to improve hyperuricemia and gouty arthritis by increasing renal excretion of uric acid and inhibiting the inflammatory cascade. Fatty acids, sterols, and terpenoids of *L. acidissima* fruit could potentially be used to treat hyperuricemia and gout arthritis. However, the proposed mechanisms require further research to confirm the potential of *L. acidissima* as a novel therapy in the prevention and treatment of hyperuricemia and gout arthritis.

## CONFLICT OF INTEREST

The authors declare no conflicts of interest.

## ACKNOWLEDGMENTS

The authors would like to thank the Pharmacology Laboratory, Faculty of Veterinary Medicine, and the Chemistry Laboratory and Biology Laboratory, Faculty of Mathematics and Natural Sciences, Syiah Kuala University, Indonesia, for the facilities provided during the research. This research was supported by research facilities and scientific and technical support from the Cibinong Advanced Characterization Laboratory – Integrated Bioproducts at the Indonesian Institute of Sciences (LIPI), the Regional Health Laboratory (Labkesda) DKI Jakarta, and the Indonesian Bioinformatics and Molecular Biology Analysis Service (Inbio). This research was funded by Direktorat Riset, Teknologi dan Pengabdian Kepada Masyarakat. Direktorat Jenderal Pendidikan Tinggi, Riset dan Teknologi. Kementerian Pendidikan, Kebudayaan, Riset dan Teknologi, grant number: 062/E5/PG.02.00.PL/2023.

## REFERENCES

Ahmadian M, Suh JM, Hah N, Liddle C, Atkins AR, Downes M, Evans RM (2013) PPARγ signaling and metabolism: The good, the bad and the future. Nat Med 19(5): 557–566. https://doi.org/10.1038/nm.3159

Ahmed AR, Lappin D (2018) Oral alkali therapy and the management of metabolic acidosis of chronic kidney disease: A narrative literature review. World J Nephrol 7(6): 117–122. https://doi.org/10.5527/wjn.v7.i6.117

Alghamdi Y, Soliman MM, Nassan MA (2020) Impact of lesinurad and allopurinol on experimental hyperuricemia in mice: Biochemical, molecular and immunohistochemical study. BMC Pharmacol Toxicol 21(1): 10. https://doi.org/10.1186/s40360-020-0386-7

Andalia N, Salim MN, Saidi N, Ridhwan M, Iqhrammullah M, Balqis U (2022) Molecular docking reveals phytoconstituents of the methanol extract from *Muntingia calabura* as promising α-glucosidase inhibitors. Karbala Int J Mod Sci 8(3): 330–338. https://doi.org/10.33640/2405-609X.3236

Andriana Y, Xuan TD, Quy TN, Minh TN, Van TM, Viet TD (2019) Antihyperuricemia, antioxidant, and antibacterial activities of *Tridax procumbens* L. Foods 8(1): 21. https://doi.org/10.3390/foods8010021

Bagul V, Dhabekar S, Sansarode S, Dandekar S (2019) Wood apple (*Limonia acidissima* L.): A multipurpose herb in cosmetics. Int J Sci Eng Develop Res 4(7): 172–181.

Cabău G, Crișan TO, Klück V, Popp RA, Joosten LAB (2020) Urate-induced immune programming: Consequences for gouty arthritis and hyperuricemia. Immunol Rev 294(1): 92–105. https://doi.org/10.1111/imr.12833

Chen Y, Chen X, Xiang T, Sun B, Luo H, Liu M, Chen Z, Zhang S, Wang C (2016) Total saponins from *Dioscorea septemloba* Thunb reduce serum uric acid levels in rats with hyperuricemia through OATP1A1 up-regulation. J Huazhong Univ Sci Technol [Med Sci] 36(2): 237–242. https://doi.org/10.1007/s11596-016-1573-z

Cui D, Liu S, Tang M, Lu Y, Zhao M, Mao R, Wang C, Yuan Y, Li L, Chen Y, Cheng J, Lu Y, Liu J (2020) Phloretin ameliorates hyperuricemia-induced chronic renal dysfunction through inhibiting NLRP3 inflammasome and uric acid reabsorption. Phytomedicine 66: 153111. https://doi.org/10.1016/j.phymed.2019.153111

de Souza CO, Valenzuela CA, Baker EJ, Miles EA, Rosa Neto JC, Calder PC (2018) Palmitoleic acid has stronger anti-inflammatory potential in human endothelial cells compared to oleic and palmitic acids. Mol Nutr Food Res 62(20): 1800322. https://doi.org/10.1002/mnfr.201800322

Gharbieh EA, Shehab NG, Lmasri IM, Bustanji Y (2018) Antihyperuricemic and xanthine oxidase inhibitory activities of *Tribulus arabicus* and its isolated compound, ursolic acid: *In vitro* and *in vivo* investigation and docking simulations. PLoS One 13(8): e0202572. https://doi.org/10.1371/journal.pone.0202572

Hambal M, Frengki F, Sari WE, Vanda H (2022) *In silico* prediction of flavan-3-ol as a bioactive compound of *Calophyllum macrophyllum* as a potential drug against angiostrongylus eosinophilic meningitis. Vet World 15(5): 1305–1313. https://doi.org/10.14202/vetworld.2022.1305-1313

Huang R, Zhang C, Wang X, Hu H (2021) PPARγ in ischemia-reperfusion injury: Overview of the biology and therapy. Front Pharmacol 12: 600618. https://doi.org/10.3389/fphar.2021.600618

Ikhsan I, Yusnaini R, Nasution R, Munawar AA, Idroes R (2021) Application of near-infrared spectroscopy and chemometric (PCA) in variety *Holothuria atra* and *Holothuria scabra* in Simeuleu, Aceh province. IOP Conf Ser: Mater Sci Eng 1087(1): 012054. https://doi.org/10.1088/1757-899x/1087/1/012054

Ismail M, Sajid H, Khan F, Mohammed MHN (2019) Management of rheumatology disorders and the pharmacist's role: Gout and related disorders. In: Encyclopedia of Pharmacy Practice and Clinical Pharmacy. Amsterdam: Elsevier, pp. 519–536. https://doi.org/10.1016/B978-0-12-812735-3.00533-1

Jenecius A, Uthayakumari F, Mohan V (2012) GC-MS determination of bioactive components of *Sauropus bacciformis* Blume (Euphorbiaceae). J Curr Chem Pharm Sci 2(4): 347–358.

Ko SNN, Naing HH (2020) Nutritional compositions, antioxidant and antimicrobial activities of exotic nutritional compositions, antioxidant and antimicrobial activities of exotic fruit *Limonia acidissima* L. 3rd Myammar Korea Conf Res J 3(3): 798–805.

Lamani S, Anu-Appaiah KA, Murthy HN, Dewir YH, Rihan HZ (2021) Fatty acid profile, tocopherol content of seed oil, and nutritional analysis of seed cake of wood apple (*Limonia acidissima* L.), an underutilized fruit-yielding tree species. Horticulturae 7(9): 275. https://doi.org/10.3390/horticulturae7090275

Libório G, Costa A, Buccini DF, Lucia A, Arruda A, Favaro, SP, Moreno SE (2020) Phytochemical profile, anti-inflammatory, antimutagenic and antioxidant properties of *Acrocomia aculeata* (Jacq.) Lodd. pulp oil. Food Sci Technol, Campinas 40(4): 963–971. https://doi.org/10.1590/fst.25319

Lin Y, Liu PG, Liang WQ, Hu YJ, Xu P, Zhou J, Pu JB, Zhang HJ (2018) Luteolin-4′-O-glucoside and its aglycone, two major flavones of *Gnaphalium affine* D. Don, resist hyperuricemia and acute gouty arthritis activity in animal models. Phytomedicine 41: 54–61. https://doi.org/10.1016/j.phymed.2018.02.002

Lipinski CA (2004) Lead- and drug-like compounds: The rule-of-five revolution. Drug Discov Today Technol 1(4): 337–341. https://doi.org/10.1016/j.ddtec.2004.11.007

Meng Q, Feng Z, Zhang X, Hu L, Wang M, Zhang H, Li S (2019) PPAR-γ activation exerts an anti-inflammatory effect by suppressing the NLRP3 inflammasome in spinal cord-derived neurons. Mediators Inflamm 2019: 6386729. https://doi.org/10.1155/2019/6386729

Müller DSMC, Coelho GB, Carolina M, Michel DP, Saúde-Guimarães DA (2019) *Lychnophora pinaster* ethanolic extract and its chemical constituents ameliorate hyperuricemia and related inflammation. J Ethnopharmacol 242: 112040. https://doi.org/10.1016/j.jep.2019.112040

Muzio G, Barrera G, Pizzimenti S (2021) Peroxisome proliferator-activated receptors (PPARs) and oxidative stress in physiological conditions and in cancer. Antioxidants 10(11) 1734. https://doi.org/10.3390/antiox10111734

Ni Q, Lu X, Chen C, Du H, Zhang R (2019) Risk factors for the development of hyperuricemia. Medicine 98(42): e17597. https://doi.org/10.1097/MD.0000000000017597

Palomer X, Pizarro-Delgado J, Barroso E, Vázquez-Carrera M (2018) Palmitic and oleic acid: The yin and yang of fatty acids in type 2 diabetes mellitus. Trends Endocrinol Metab 29(3): 178–190. https://doi.org/10.1016/j.tem.2017.11.009

Purnama A, Mardina V, Puspita K, Qanita I, Rizki DR, Hasballah K, Iqbal M, Sarong M (2021) Molecular docking of two cytotoxic compounds from *Calotropis gigantea* leaves against therapeutic molecular target of pancreatic cancer. Narra J 1(2): e37. https://doi.org/10.52225/narraj.v1i2.37

Purnama A, Rizki DR, Qanita I, Iqhrammullah M, Ahmad K, Mardina V, Puspita K, Hasballah K (2022) Molecular docking investigation of calotropone as a potential natural therapeutic agent against pancreatic cancer. J Adv Pharm Technol Res 13(1): 44–49. https://doi.org/10.4103/japtr.japtr_143_21

Rakhunde PB, Saher S, Ali SA (2014) Neuroprotective effect of *Feronia limonia* on ischemia reperfusion induced brain injury in rats. Indian J Pharmacol 46(6): 617–621. https://doi.org/10.4103/0253-7613.144920

Salehi B, Azzini E, Zucca P, Varoni EM, Kumar NVA, Dini L, Panzarini E, Rajkovic J, Fokou PVT, Peluso I, Mishra AP, Nigam M, El Rayess Y, El Beyrouthy M, Setzer WN, Polito L, Iriti M, Sureda A, Quetglas-Llabrés MM, Martorell M, Martins N, Sharifi-Rad M, Estevinho LM, Sharifi-Rad J (2020) Plant-derived bioactives and oxidative stress-related disorders: A key trend towards healthy aging and longevity promotion. Appl Sci 10(3): 947. https://doi.org/10.3390/app10030947

Serrano JL, Figueiredo J, Almeida P, Silvestre S (2020) From xanthine oxidase inhibition to *in vivo* hypouricemic effect: An integrated overview of *in vitro* and *in vivo* studies with focus on natural molecules and analogues. Evid Based Complement Alternat Med 2020: 9531725. https://doi.org/10.1155/2020/9531725

Srinivasan P, Deivamarudachalam TPD, Vellingiri M, Castro J, Jaganathan D, Kanagarajan M (2015) *Limonia acidissima* L. (wood apple) as feed additive enhanced growth performance, immune response and disease resistance of Indian Major Carp, Catla Catla (Ham.) against *Aeromonas hydrophila* infection. Int Res J Pharm 6(2): 143–152. https://doi.org/10.7897/2230-8407.06232

Srivastava R, Mishra N, Agarwal S, Mishra N (2019) Pharmacological and phytochemical properties of kaitha (*Feronia limonia* L.): A review. Plant Arch 19(suppl. 1): 608–615.

Stewart DJ, Langlois V, Noone D (2019) Hyperuricemia and hypertension: Links and risks. Integr Blood Press Control 12: 43–62. https://doi.org/10.2147/IBPC.S184685

Strilchuk L, Fogacci F, Cicero AF (2019) Safety and tolerability of available urate-lowering drugs: A critical review. Expert Opin Drug Saf 18(4): 261–271. https://doi.org/10.1080/14740338.2019.1594771

Sungthong B, Manok S, Sato H, Sato VH (2016) Effects of *Aquilaria crassna* on xanthine oxidase activity *in vitro* and hyperuricemic mice. Indian J Pharm Sci 78(4): 547–552. https://doi.org/10.4172/pharmaceutical-sciences.1000151

Susanty A, Dachriyanus, Yanwirasti, Wahyuni FS, Amelia P, Frengki, Ikhtiarudin I, Hirasawa Y, Kaneda T, Morita H (2021) Cytotoxic activity and molecular docking of indole alkaloid voacangine, bis-indole alkaloids vobtusine, and vobtusine lactone from the Indonesian plant: *Voacanga foetida* (Blume) Rolfe. Indones J Pharm 32(4): 442–453. https://doi.org/10.22146/ijp.1250

Suyanto A, Noor E, Rusli MS, Fahma F (2022) Improvement yield of applewood (*Feronia limonia*) flavor extract by liquid-liquid extraction with dichloromethane solvent. Food Sci Technol (Campinas) 42: e47520. https://doi.org/10.1590/fst.47520

Tallei TE, Tumilaar SG, Lombogia LT, Adam AA, Sakib SA, Emran TB, Idroes R (2021) Potential of betacyanin as inhibitor of SARS-CoV-2 revealed by molecular docking study. IOP Conf Ser: Earth Environ Sci 711: 012028. https://doi.org/10.1088/1755-1315/711/1/012028

Tseuguem PP, Nguelefack TB, Piégang BN, Mbankou Ngassam S (2019) Aqueous and methanol extracts of *Paullinia pinnata* (Sapindaceae) improve monosodium urate-induced gouty arthritis in rat: analgesic, anti-inflammatory, and antioxidant effects. Evid Based Complement Alternat Med 2019: 5946291. https://doi.org/10.1155/2019/5946291

Vijayvargia P, Vijayvergia R (2014) A review on *Limonia acidissima* L.: Multipotential medicinal plant. Int J Pharm Sci Rev Res 28(1): 191–195.

Wang R, Ma C, Zhou F, Kong L (2016) Siwu decoction attenuates oxonate-induced hyperuricemia and kidney inflammation in mice. Chin J Nat Med 14(7): 499–507. https://doi.org/10.1016/S1875-5364(16)30059-0

Wang X, Deng J, Xiong C, Chen H, Zhou Q, Xia Y, Shao X, Zou H (2020) Treatment with a PPAR-γ agonist protects against hyperuricemic nephropathy in a rat model. Drug Des Devel Ther 14: 2221–2233. https://doi.org/10.2147/DDDT.S247091

Wu Z, Xue Q, Zhao Z, Zhou PJ, Zhou Q, Zhang Z, Deng JP, Yang K, Fan H, Wang YF, Wang ZP (2019) Suppressive effect of huzhentongfeng on experimental gouty arthritis: An *in vivo* and *in vitro* study. Evid Based Complement Alternat Med 2019: 2969364s. https://doi.org/10.1155/2019/2969364

Yong T, Chen S, Xie Y, Chen D, Su J, Shuai O, Hu H, Zuo D, Liang D (2018) Hypouricemic effects of *Armillaria mellea* on hyperuricemic mice regulated through OAT1 and CNT2. Am J Chin Med 46(3): 585–599. https://doi.org/10.1142/S0192415X18500301

Yusnaini R, Ikhsan I, Idroes R, Munawar AA, Arabia T, Saidi N, Nasution R (2021) Near-infrared spectroscopy (NIRS) as an integrated approach for rapid classification and bioactive quality evaluation of intact *Feronia limoni*. IOP Conf Ser: Earth Environ Sci 667: 012028. https://doi.org/10.1088/1755-1315/667/1/012028

Yusnaini R, Nasution R, Saidi N, Arabia T, Idroes R, Ikhsan I, Bahtiar R, Iqhrammullah M (2023) Ethanolic extract from *Limonia acidissima* L. fruit attenuates serum uric acid level via URAT1 in potassium oxonate-induced hyperuricemic rats. Pharmaceuticals 16(3): 419. https://doi.org/10.3390/ph16030419

Zhu L, Dong Y, Na S, Han R, Wei C, Chen G (2017) Saponins extracted from *Dioscorea collettii* rhizomes regulate the expression of urate transporters in chronic hyperuricemia rats. Biomed Pharmacother 93: 88–94. https://doi.org/10.1016/j.biopha.2017.06.022.

**AUTHOR CONTRIBUTION:**

| Contribution | Yusnaini R | Ikhsan | Nurman S | Idroes R | Arabia T | Saidi N | Nasution R |
|---|---|---|---|---|---|---|---|
| Concepts or ideas | x | x | x | x | x | x | x |
| Design | x | x | x | x | x | x | x |
| Definition of intellectual content | x | x | | x | x | x | x |
| Literature search | x | x | x | x | x | x | x |
| Experimental studies | x | x | | | x | x | x |
| Data acquisition | x | x | x | x | x | x | x |
| Data analysis | x | x | x | x | x | x | x |
| Statistical analysis | x | x | x | x | x | x | x |
| Manuscript preparation | x | | | x | x | x | x |
| Manuscript editing | x | x | x | x | x | x | x |
| Manuscript review | x | x | x | x | x | x | x |

**Citation Format:** Yusnaini R, Ikhsan, Nurman S, Idroes R, Arabia T, Saidi N, Nasution R (2023) Predicting anti-hyperuricemic and anti-gouty activities of fatty acids from *Limonia acidissima* L. fruit: *In silico-in vivo* study. J Pharm Pharmacogn Res 11(5): 757–774. https://doi.org/10.56499/jppres23.1652_11.5.757

**Supplementary material**

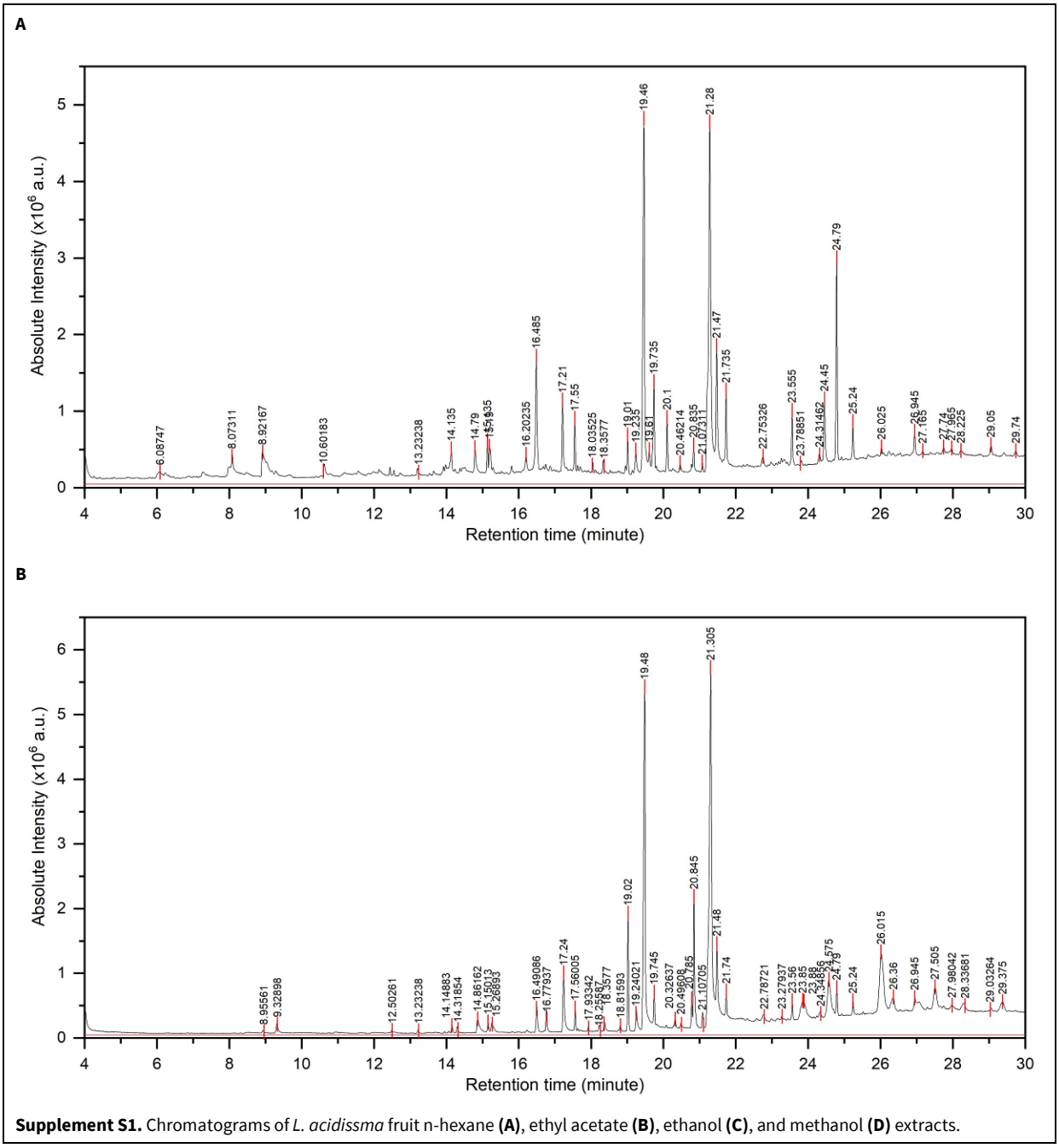


**Supplement S1.** Chromatograms of *L. acidissma* fruit n-hexane **(A)**, ethyl acetate **(B)**, ethanol **(C)**, and methanol **(D)** extracts.

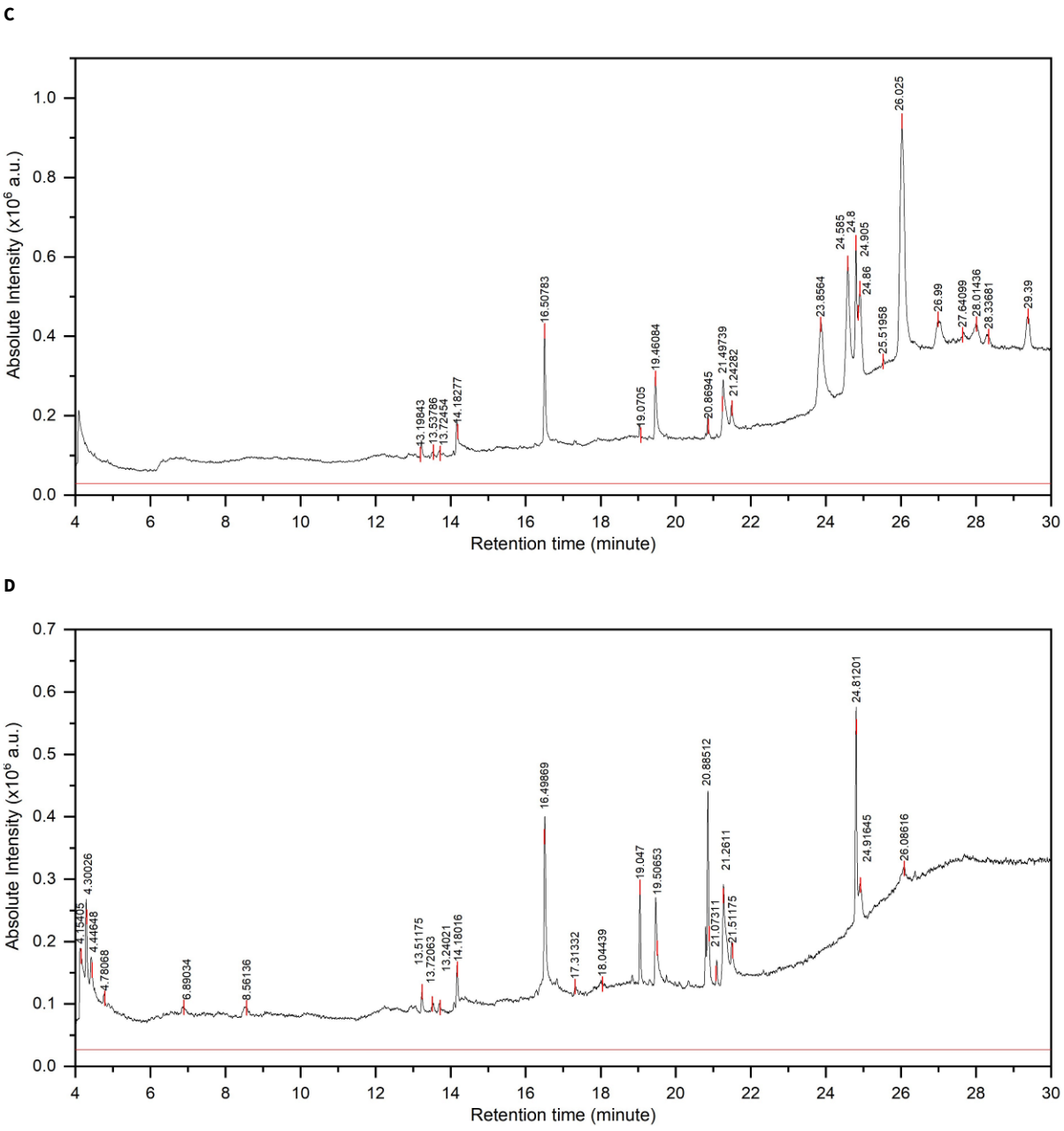


**Figure S1.** Chromatograms of *L. acidissma* fruit n-hexane **(A)**, ethyl acetate **(B)**, ethanol **(C)**, and methanol **(D)** extracts (continued…)